

DESIGN OF A NOVEL DEVICE FOR CARBURIZING REGULATION

Philippe JACQUET^{1*}, Daniel R. ROUSSE²
Gilles Bernard¹, Michel LAMBERTIN¹

¹ LABOMAP, Ecole Nationale Supérieure d'Arts et Métiers,
71 250 Cluny, France
Tel : 33 03 85 59 53 28 ; Fax : 33 03 85 59 53 70
jacquet@cluny.ensam.fr

² Département de génie mécanique, Université Laval,
Sainte-Foy (Québec), Canada G1K 7P4
Tel : 001 418 656 2131 (3345) ; Fax : 001 418 656 7415
Daniel.Rousse@gmc.ulaval.ca

* *Author to whom further correspondence should be addressed.*

ABSTRACT

This paper presents the principle and testing of a novel device developed for vacuum furnace applications. The experimental device is made of a thin iron foil with a carburizing atmosphere on one side and a decarburizing atmosphere on the other. The principle of carburizing control is based on the fact that when steady state of carbon diffusion is reached across the thin iron foil, the measured mass flux of carbon on the decarburizing side is related to the inflow of carbon into the parts during the carburizing treatment. Hence, as a probe could be inserted directly into a given furnace, it would provide an *in-situ* control facility. The proposed device could than be used for controlling low-pressure or vacuum carburizing treatments. The results presented here are limited to atmospheric conditions. However, they gave the incentive to the researchers to pursue the development of the device to allow for measurements in a low-pressure furnace.

Key words : **carburizing, sensor, control, iron foil**

NOMENCLATURE

C	Carbon concentration, %
D	Mass diffusion coefficient, cm^2/s
E	Potential, V
I	Intensity, A
J	Conversion factor, 4,19 J/Cal
K	Mass transfer coefficient, cm/s
L	Foil thickness, μm
G	Cell factor
\dot{m}	Mass flow rate, mg/h
Q	Activation energy, J/mol
R	Constant, 8.314 J/mol K
R_o	Electric resistance at 0°C , Ω
t	Time, s, min, h
T	Temperature, K

Greek symbols

α	Temperature correction coefficient
χ	Mole fraction of the specie in the gas
λ_s	Thermal conductivity of the specie, W/m K
λ_G	Thermal conductivity of the gas, W/m K
Δe	Signal of the catharometer, V

Indices and superscripts

0	Reference condition
a	Related to the gas activation energy
C	Carburizing
d	Related to the solid activation energy, diffusion
D	Decarburizing
i	Gas-solid interface
P	Carbon potential
s	Saturation
t	Transition in the chamber

1. INTRODUCTION

Although heat treatments of iron and steel have been done for over 3000 years, it is only since the last decade that several regulation processes have been available for the regulation of atmospheric carburizing treatments. Many of these rely on devices that monitor the carbon potential (concentration) at atmospheric pressure in the furnaces [1,2]. If any problem occurs, such as a temperature or a pressure drop, the device sends a signal to the regulation program in order to change the length of the cycle or the composition of the atmosphere [3-5]. The use of such regulation systems allows for more homogeneous carbide layers and overall control of the process.

However, to the best knowledge of the authors, no such regulation process has been made available in the context of low pressure carburizing treatments. To date, none of the existing devices that monitor the carbon potential at atmospheric pressure can be used under low-pressure conditions. This is usually due to the absence of thermodynamic equilibrium [6-7]. As a result, the low pressure carburizing processes is solely modeled by computer [8-12]. Hence, although low pressure carburizing can be more efficient than atmospheric carburizing, the lack of appropriate regulation devices seems to stand in the way of its development.

In this context, this paper presents a novel device designed, constructed and tested to bridge the gap between this need for regulation in low-pressure atmospheres and the increased performance of carburizing in such conditions.

This paper first introduces the physics of carburizing, the mathematical model, and low-pressure carburizing. Then it presents the proposed regulation device along with several details on the experimental apparatus. The following section focuses on experimental results while the last section summarizes the main conclusions and formulates a few recommendations.

2. CARBURIZING PROCESS

2.1 Physics of carburizing

The physics of carbon diffusion as applied to the proposed device is schematically shown in Figure 1. In this figure, the left side of a thin iron foil is exposed to a carburizing furnace atmosphere while the right side of this thin foil is exposed to a controlled decarburizing environment. Figure 1 indicates that propane, C_3H_8 , has been used with the proposed experimental apparatus. The principle of control is based on the fact that when steady state is reached in the iron foil, the measured mass flux of carbon on the right side is related to the inflow of carbon into the parts during the carburizing treatment. Hence, as a probe can be inserted directly into the furnace, it provides an *in-situ* control facility. Figure 1 also schematically shows that if the saturation concentration of carbon, C_s , is reached within the foil, precipitation of carbides (Fe_3C) will occur. On the other hand, if the foil is not quenched, when the carbon concentration decreases below C_s , the carbides will be dissolved within the foil.

2.2 Mathematical description of carbon diffusion

The basis for modeling single phase carburizing is the following mass balance equation which states that the total carbon in a differential volume changes in time according to the divergence of the carbon flux plus a volumetric source term of carbon that accounts for carbide precipitation or dissolution:

$$\frac{\partial C(x,t)}{\partial t} = \frac{\partial}{\partial x} \left(D(x,t) \frac{\partial C(x,t)}{\partial x} \right) + S_c(x,t); 0 \leq x \leq L; t > 0 \quad (1)$$

in which x is the distance from the carburizing surface, L is the foil thickness, C is the carbon concentration, D is the mass diffusion coefficient, and S_c is the volumetric source of carbon (it is negative in the case of carbides precipitation and positive when carbides are dissolved in the matrix). The boundary and initial conditions are:

$$K_C(t)(C_p - C(x,t)) = -D(x,t) \frac{\partial C(x,t)}{\partial x}; \quad x=0; \quad t>0 \quad (2)$$

$$K_D(t)(C(x,t) - C_G) = -D(x,t) \frac{\partial C(x,t)}{\partial x}; \quad x=L; \quad t>0 \quad (3)$$

$$C(x,0) = C_i; \quad 0 \leq x \leq L; \quad t=0 \quad (4)$$

where K_C is the mass transfer coefficient on the carburizing side, K_D is the mass transfer coefficient on the decarburizing side, C_p is the carbon potential of the carburizing atmosphere, C_G is the carbon potential of the decarburizing gas, $C_G = 0$, and C_i is the initial concentration of carbon in the material. C_i could be a function of x but for this application the initial carbon concentration is uniform throughout the foil.

The expressions for D and K have been correlated by several authors for different steels. Ghiglione [13] proposes a review that involves 13 different expressions for D and 9 for K . Here, the following forms are assumed [7]:

$$D(t) = D_0(C) \exp\left(-\frac{Q_d}{RT}\right) \quad (5)$$

$$K_D(t) = K_{D,0} \exp\left(-\frac{Q_a}{RT}\right) \quad (6)$$

in which Q_d is the activation energy of carbon diffusion in austenite, Q_a is the activation energy of the carburizing atmosphere, $R=8.314$ J/mol K, and T is the temperature in Kelvin.

2.3 Low pressure carburizing

The first step in a low pressure carburizing treatment is pumping. This is followed by a heating phase of the workload in a nitrogen atmosphere or in a vacuum. This oxygen free atmosphere allows to eradicate the risk of internal intergranular oxidation. Moreover, the total carburizing cycle time is reduced compared to standard atmospheric carburizing.

In a furnace operating with «boost-diffusion» steps, when the appropriate carburizing temperature is reached (around 1000°C), the carburizing gas (in this case propane C_3H_8 or ethylene C_2H_4) is introduced at a pressure of 6 mbar. The vacuum pump regulates the operating pressure. In such conditions, the surface of the steel workload is quickly saturated with carbon atoms. This leads to the diffusion of carbon in the matrix and hence to the formation of a carburized layer. Care as to be taken to avoid sooting: injection of the carburizing gas has to be stopped in time. In this respect, the pump evacuates the gas while the temperature remains constant for the subsequent diffusion step. Generally, the deeper the required carburizing depth, the greater the needed number of boost-diffusion steps [14]. Figure 2 presents a typical vacuum carburizing cycle with four «boost-diffuse» steps. Figure 2 indicates that about 20 minutes were required to pump under 10^{-1} mbar (thin line). Hence, the residual oxygen is not sufficient to oxidize the workload. Then, convective heat transfer with nitrogen enhances heat transfer to the workload. When the temperature reaches about 600°C (thick line), the nitrogen atmosphere is removed and heating is ensured solely by radiation. Approximately 90 minutes were needed to reach about 1000°C. Then started the carburizing cycles.

3. EXPERIMENTAL APPARATUS

The principle described in the previous section had to be validated carefully before any application to a real furnace be considered. Hence, the first sets of experiments were carried out at atmospheric pressure. For these experiments, a laboratory experimental apparatus was designed and built. It is schematically illustrated in Figure 3. In this figure, the experimental cell① is located in a thermally controlled environment②. In the center of this cell① a thin iron foil③ is installed creating two chambers④⑤ which reproduce the configuration of Figure 1. On the left side④ a mixture of nitrogen and carburizing gas⑦ is introduced, and on the right side⑤ the decarburizing gas (hydrogen⑧ and water vapor⑨) is circulated. The outflow of decarburizing gas is analyzed by a catharometer⑩ [7]. An infrared gas analyzer could also be used.

The catharometer, used for the gas analysis, involves a Wheatstone bridge with a reference flow on one side and the decarburizing flow^⑩ on the other side. Once carbon atoms emerge from the right surface of the foil^③, the decarburizing reactions produce carbon monoxide, CO, and methane, CH₄ in the chamber^⑤. These new substances influence the overall conductivity of the gas mixture and induce a potential in the catharometer. Hence, the increase of the catharometer signal indicates that new types of molecules have appeared in the decarburizing outflow^⑩ due to the decarburizing reaction. The sensitivity of the catharometer is given by [7]:

$$\Delta e = \left[\frac{1}{G} \right] \left[\frac{\alpha R_o EI^2}{4J} \right] \chi \left(\frac{1}{\lambda_s} - \frac{1}{\lambda_G} \right) \quad (7)$$

In this study $E=12V$, $I=250mA$, and $\alpha R_o=48\Omega$. The thermal conductivity of the specie at 300K (which is a combination of carbon monoxide, CO, and methane, CH₄) is taken as that of methane, $\lambda_s=34,26$ W/mK, and the decarburizing gaz conductivity is that of hydrogen, $\lambda_G=186,86$ W/mK (here the water content is neglected) [15]. The cell factor has been evaluated with a hydrogen flow and a hydrogen-vapor flow [7] to yield, $G=1,4 \times 10^4$. Hence, Eq.7 becomes:

$$\Delta e = 1,52 \chi \quad (8)$$

which yields the relationship between the signal and the mole fraction of carbon in the decarburizing gas.

Provided that the total mass flow rate of decarburizing gas, \dot{m}_G , is known, it is possible to use Eq.8 to obtain the mass flow rate of carbon:

$$\dot{m}_c = \frac{\Delta e \dot{m}_G}{(1,52 - \Delta e)} \quad (9)$$

Then, the mass flow rate of carbon is divided by the surface area of the foil to yield the mass flux of carbon.

4. RESULTS

Experiments were first carried out with the use of the above-mentioned experimental apparatus (section 3) to establish whether or not the principle could indeed be used to control low-pressure carburizing processes.

4.1 Foil thickness

The first series of test (figure 4) was carried out to determine the appropriate foil thickness of the proposed probe. A thin foil will lag less than a thicker foil as the diffusion is not instantaneous. However, the foil has to be thick enough to ensure acceptable mechanical properties. Steady state conditions may be reached faster with a thin foil than with a thicker foil but the suggested probe has to be robust enough for use in an industrial furnace.

Six foil thicknesses were tested namely: $L = 25 \mu m, 40 \mu m, 70 \mu m, 100 \mu m, 120 \mu m, 180 \mu m$. For all tests involved in this section, the decarburizing atmosphere^⑤ consisted of pure hydrogen (no water vapor) and injection in the carburizing chamber^④ ($12s \pm 1s$) started after $20s \pm 1s$ of acquisition time. Physically, soon after the injection the surface concentration reaches C_s on the carburizing side^④. This surface concentration is maintained until injection is stopped. In the vicinity of the surface^④, carbides begin to precipitate in the matrix and the carbon concentration reaches saturation deeper and deeper in the foil^③. Then, when the injection is stopped, the concentration decreases below C_s and carbides begins to dissolve in the matrix^③. This explains the two slopes visible (mostly for the thin foils) in figure 4.

Figure 4 immediately reveals that: (1) as the thickness of the foil increases, the response time of the detector augments, and (2) as the thickness increases the maximum value of the signal decreases.

Response time: The measured response time t is the sum of: (1) the diffusion time t_d , (2) the reaction time at the interfaces t_i , (3) the sensitivity time t_s , and (4) the transition time t_t . The time t_d is the quantity of interest while t_t depends of the geometry and the gas flow rate. t_i is a constant evaluated with a perforated

foil and measured between the moment the valve is opened and the detection by the catharometer: $t_r = 14s$. t_i is the sorption and desorption reaction time at both gas-solid interfaces, it is assumed negligible compared to t_r . t_s is the time lag between the methane formation on the decarburizing side and the detection by the catharometer. The catharometer possesses a sensitivity threshold under which it cannot detect the presence of carbon. However, t_s has been found negligible compared to t_r . Table 1 indicates explicitly the diffusion times obtained with the apparatus.

Table 1: Diffusion time as a function of the foil thickness.

Thickness[μm]	Diffusion time [s]
25	10.8
40	13.9
70	25.0
100	41.1
120	53.2
180	117.0

Amplitude of the signal: A constant signal indicates a constant decarburizing flow rate. Grabke [16] mentions that this decarburizing flow rate is not a function of the carbon content of the steel. This leads to the conclusion that the flow rate is limited by diffusion and hence by the thickness of the foil. Figure 4 clearly indicates this trend although quasi steady state is reached. Steady state can not be obtained with the proposed settings as the carburizing is stopped after $12s \pm 1s$. Hence, the concentration of carbon on the left surface of the foil (figure 1) will not be constant in time after injection is over. Table 2 shows the relation between the mass flux of carbon (converted signal of the catharometer) and the foil thickness.

Table 2: Mass flow rate of carbon as a function of the foil thickness.

Thickness[μm]	Mass flux [mg/h/cm^2]
25	1.06E-01
40	8.46E-02
70	4.23E-02
100	1.90E-02
120	1.41E-02
180	7.75E-03

The table indicates that the mass flux of carbon is approximately inversely proportional to the foil thickness although steady state is not maintained. Here, the mass fluxes are low as the mass flux of decarburizing gas was low ($53,50 \text{ mg/h/cm}^2$) and the dew point very low (dry hydrogen has been used, dew point = -40°C).

After several tests, $70 \mu\text{m}$ was found to be the optimal thickness as it is tough enough to ensure reliability and appropriate mechanical properties: thicker foils are not responding fast enough to ensure an adequate control. The following results are all presented for $70 \mu\text{m}$ thick foils.

4.2 Carburizing mixture concentration

The obtaining of the optimal carburizing gas concentration to yield the maximum mass flow rate of carbon through the foil was considered next. Experiments proceeded by reducing the concentration of carburizing gas from 18% to 0,4% to detect the threshold indicating this optimal concentration. In this series of test, the foil was carburized during $23s \pm 1s$ for each experience. Figure 5 indicates that the valve was opened $200s \pm 1s$ after acquisition started. Typically, concentrations of propane above 2,0% yielded no different maximum mass flow rates of carbon: for high concentrations, the responses of the catharometer were identical. With too high a concentration, the mixture is overcarburizing and the excess carbon precipitates as carbides in the matrix; with too low concentration, the carburizing rate is reduced. For the threshold concentration, the gas concentration in the left enclosure is just high enough to yield a surface concentration of carbon nearly equal to C_s . This indicates that a rich mixture is not required to ensure the maximum mass flow and that, at least in principle, the proposed device could be used to calibrate the appropriate gas concentration. Figure 5 shows sample results for concentrations below the threshold. In

this case, absorption of carbon at the steel's surface (the carbon potential, C_p) becomes the limiting step; the mass transfer coefficient, K_C , is not the limiting parameter here as the slope of the curves are all similar.

In a furnace, once the optimum concentration of carburizing gas (the carbon potential, C_p) has been determined, it is possible to increase the carburizing period until steady-state is achieved. In this case, the absorption rate of carbon at the steel's surface and the diffusion rate are approximately equal. It is also possible to increase the mass flow rates of carburizing species ⑦ to make sure that the mass transfer coefficient, K_C , is not the limiting parameter.

For the mass flow rates of carburizing mixture involved for this particular cell test①, a propane concentration above 2% was required to maximize the mass flow rate of carbon.

4.3 Dew point of the decarburizing mixture

The decarburizing gas is a mixture of hydrogen⑧ and water vapor⑨ with a composition that should be calibrated to ensure a maximum decarburizing potential without the risk of oxidation. In fact, two alternatives could be considered to increase decarburizing rates: an increase of the mass flow rate and/or an injection of water vapor in the hydrogen. Bracho-Troconis [18] investigated the effect of the mass flow rate of decarburizing gas on the decarburizing rates for given water content (dew point at -20°C). Here, the effects of the variation of the dew point of the mixture are investigated. An important increase of the mass flow rate of hydrogen would lead to a lower sensitivity of the catharometer which is an undesirable effect.

Figure 6 reports the effects of the dew point of the mixture on the mass flux of carbon (signal of the catharometer) for a constant decarburizing gas flux⑧⑨ of 157.36 mg/h/cm^2 . Injection periods of $12\text{s}\pm 1\text{s}$ were considered for each experiment. Figure 6 shows two things: (1) the maximum mass flux increases with the water content as a second decarburizing reaction occurs at the interface: $C+H_2O\rightarrow CO+H_2$; and (2) the rate at which carbon is removed after injection is stopped is also more important with increasing water content (the signal gets back to zero faster when the water content is important). In fact, the second reaction ($C+H_2O\rightarrow CO+H_2$) becomes preponderant over the combination of hydrogen and carbon into methane. Indeed, Grabke [17] showed that for dew points above 7°C , the reaction rate due to hydrogen is negligible compared to that due to water vapor. However, the dew point should not be too high to avoid the risk of oxidation. In the following tests, a mixture with a dew point of about 0°C (corresponding to a water vapor partial pressure of 3,3 Pa) has been used [17].

For the results presented in figure 6, the area under each curve is identical (within experimental uncertainty) as the total amount of carbon introduced by the carburizing process is similar in each case. The injection period is the same for the three cases.

4.4 Carburizing period

The fourth parameter to be studied was the length of the period of the «boost-diffusion» carburizing step. As shown in Figure 7, the maximum value of the mass flow rate of carbon is similar for all carburizing periods from $10\text{s}\pm 1\text{s}$ to $230\text{s}\pm 1\text{s}$ provided that the same decarburizing rate was used (same mass flux and water content) and that the carburizing gas concentration was above 2% (the surface concentration of carbon equals C_s).

For this series of experiments, the peak height is determined by the decarburizing rate and is proportional to this rate. This rate is in turn a function of the mass flow rate of the hydrogen-water vapor mixture as well as its composition. Initially, the signal recorded by the catharometer is constant indicating that no carbon has crossed the foil. Then, the signal steeply increases a few seconds after the injection of the carburizing gas: the surface concentration of carbon reached C_s almost instantaneously. The response is expected to be different in a furnace or with a lower water content of the decarburizing gas as shown in Table 1 for $L=70 \mu\text{m}$.

In Figure 7, injection of carburizing mixture starts at $t = 200\text{s}\pm 1\text{s}$. Here again, the inertia of the whole apparatus has been found by subtracting the time constant ($t_t + t_s + t_i$) of the fluid flowing through the system to the total time recorded.

The surface under each curve in Figure 7 corresponds to the amount of carbon that has diffused through the foil. This quantity divided by the carburizing time and by the surface area of the foil yields the average mass flux of carbon.

The shape of the curves in Figure 7 also indicate that when the carburizing period increases, there is an increasing amount of carbide that precipitates within the foil: the area under each curve is different and the maximum flux is similar. Also, it is shown that the presence of carbide in the steel diminishes its ability to

diffuse carbon: D decreases. This is shown by the slopes of the curves after the peaks: the steeper the slope, the lower the amount of carbide provided that the carburizing period is shorter.

Figure 7 also indicates that the time required to reach the initial level (no flow rate) after carburizing is stopped increases with increasing periods. This indicates that when the carburizing period is over, the carbides start to be dissolve in the steel. When, the process is over, the carbon concentration in the foil is back to C_i . These phenomena have also been observed by Sugiyama, Ishikawa et Iwata [19].

4.5 Average mass flux of carbon

To complete the results, the average mass flux for the tested carburizing periods with overcarburizing atmosphere is reported in Table 3.

Table 3: Decarburizing time and average mass flux of carbon for several carburizing periods.

Carburizing period [s]	Decarburizing time [min]	Average mass flux [mg/h/cm ²]
10	9.2	30
25	10.8	15
35	12.3	13
45	13.0	11
70	15.1	8,6
230	17.5	3,3

The table indicates that the mass flux is very high at the beginning of the carburizing sequence, but decrease very rapidly as carbon atoms saturate the steel and form carbides that diminishes D . The results reported in table 3 compared to those in table 2 also clearly show the effects of the water content in the decarburizing mixture.

In summary this test indicates that when the atmosphere is overcarburizing, the precipitation of carbide influences the mass diffusion and that carburizing steps, along with corresponding diffusion steps, are needed to obtain a better diffusion. Hence, the carburizing atmosphere should be controlled to ensure that the surface concentration of carbon remains just below C_s . This would allow for continuous carburizing at a maximum rate without the risk of sooting. Here again, results suggest that the proposed device could be used to monitor the process.

5. CONCLUSION

5.1 Contributions

This paper presented the principle of a novel regulation device that could be used in atmospheric, low-pressure or vacuum conditions. The sample results indicate that the device could be used to monitor and control the carburizing process of steel in furnaces. It could be used to:

- study the impact of the carburizing gas mass flow rate and concentration on the mass flow rate of carbon;
- determine the appropriate decarburizing gas composition and mass flow rate on that of carbon;
- develop carburizing cycles that do not require diffusion steps;
- investigate the effect of the variation of selected parameters;
- provide data for simulation programs based on the solution of transient mass diffusion with convective boundary conditions;
- quantify the rate of carbide precipitation and dissolution with the steel matrix;
- etc.

5.2 Current work

It should now be interesting to apply the proposed principle to the design of a sensor to be used in a real furnace: this has been done but will be the subject of an upcoming publication.

Moreover, it would be relevant to obtain correlations between the mass flow rate of carbon in the sensor and that in the workload of the furnace as a function of the workload geometry and properties and the furnace configuration. This is the subject of current work by the authors: two main projects are actually underway: (1) experimental measurements in a prototype furnace; and (2) numerical simulation of the process.

6. REFERENCES

- [1] Bond, H.W., Dispositif de mesure et de régulation du potentiel carbone: vue d'ensemble et historique. *Traitement thermique*, n°235, Mars 1990, pp.29-31.
- [2] Sobusiak, T., Method of measuring carbon potential and carbon transfer coefficient. *HEAT TREATMENT SHANGAI'83*. Proceedings of the Third International Congress on Heat Treatment of Materials, 7 - 11 November 1983, Shanghai, Edited by professor T. Bell, pp.1.79-1.85.
- [3] Aubry, R., Optimisation de la cémentation gazeuse en four continu par pilotage automatique. *Traitement thermique*, n°174, Mai 1983, pp.49-63.
- [4] Lipinsky, A., and Suryan, W.L., Using programmable control systems in heat treatment processes. *HEAT TREATMENT SHANGAI'83*. Proceedings of the Third International Congress on Heat Treatment of Materials, 7 - 11 November 1983 Shanghai, Edited by professor T. Bell, pp.4.36-4.40.
- [5] Edenhofer, B., and W. Lerche, Developments in process technology and procedure of gas carburizing. *Härtereien - technische Mitteilungen*, vol. 49, n°2, pp.88-95, 1994.
- [6] Jacquet, P., Bernard, G., Jomain, B., Souchard, J.P., and Lambertin, M., Développement d'un capteur de suivi pour la cémentation basse pression des aciers, *Traitement Thermique* n°312, Novembre 1998.
- [7] Jacquet, P., Cémentation basse pression des aciers. Développement d'un capteur de suivi, Thèse ENSAM, Cluny, 1998, 144 p.
- [8] Goldstein, J.I., and Moren, A. E., Diffusion modeling of the Carburization Process, *Metallurgical transaction A*, vol. 9A, November 1978, pp. 1515-1525.
- [9] Madsac, M., Queille, P., Kostelitz, M., Prévision des profils de concentration en carbone à partir d'un modèle de cémentation gazeuse, Application à l'optimisation des cycles thermiques. *Traitement thermique*, n°174, Mai 1983, pp.19-25.
- [10] Morral, J.E., Dupen, B.M., and Law, C.C., Application of Commercial Computer Codes to the Modeling Carburizing Kinetics of Alloy Steels. *Metallurgical Transactions A*, vol. 23A, 1992, pp. 2069-2071.
- [11] Pavlossoglou, J., A new optimisation model of boost-diffusion cycle for infinite surface steel plates / cylinder to minimise time for desired carbon profile. *HEAT TREATMENT SHANGAI'83*. Proceedings of the Third International Congress on Heat Treatment of Materials, 7 - 11 November 1983 Shanghai. Edited by professor T. Bell, pp.1.86-1.96.
- [12] Stickels, C. A., Analytical Models for the Gas Carburizing Process. *Metallurgical Transactions B*, vol. 20B, 1989, pp. 535-546.
- [13] Ghiglione, D., Modèles mathématiques de cémentation, *Traitement thermique*, n°195, pp.31-39, 1985.
- [14] Deshayes, J. Germain, P. Jacquot, E. Denisse, G. Dervieux, La cémentation basse pression des aciers. *Traitement thermique*, n°261 Janvier/ Février 1993, pp.22-30.
- [15] *Handbook of Chemistry and Physics*, 55th Ed., CRC Press, Cleveland, 1975, p.E-2.
- [16] Grabke, H.J., Kinetics and mechanisms of gas-metal interactions, *Ann. Rev. Mat. Sci.*, vol.7, 1977, pp.155-178.
- [17] Béranger, G., Henry, G., and Sanz, G., *Le livre de l'acier – Technique et documentation*, Lavoisier, Paris, 1994, p.233.
- [18] Bracho-Troconis, C.B., Décarburation d'acier doux; cinétique et mécanismes d'échanges de matière (carbone) à l'interface métal-gaz dans les atmosphères complexes., Thèse UTCompiègne, Septembre 1990, p. 188.
- [19] Sugiyama, M., Ishikawa, K., Iwata, H., Using Acetylene for Superior Performance Vacuum Carburizing, *Proc. 18th Conf. Heat Treating*, 12-15 october 1998, pp.49-56.

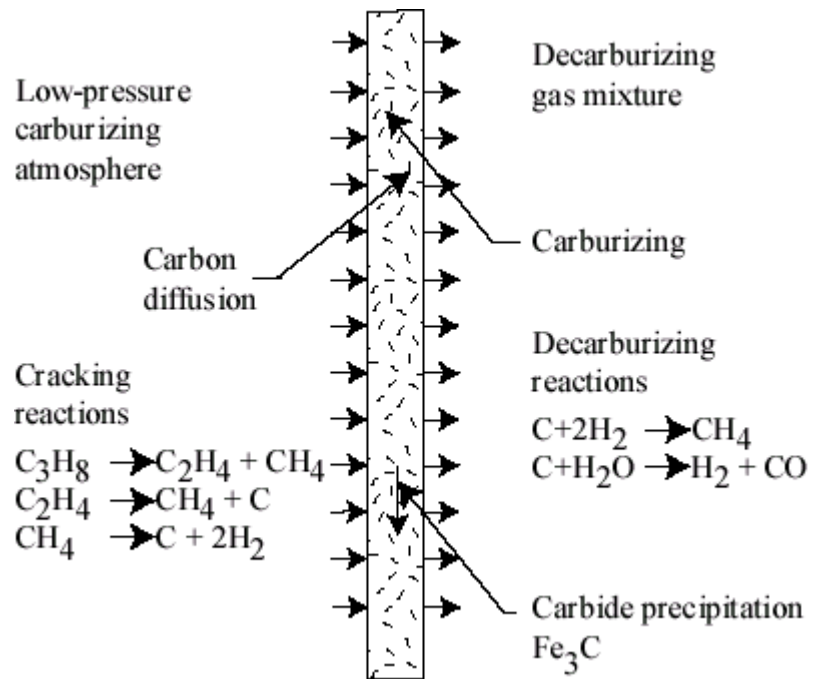


Figure 1: Schematic of carbon diffusion and carburizing.

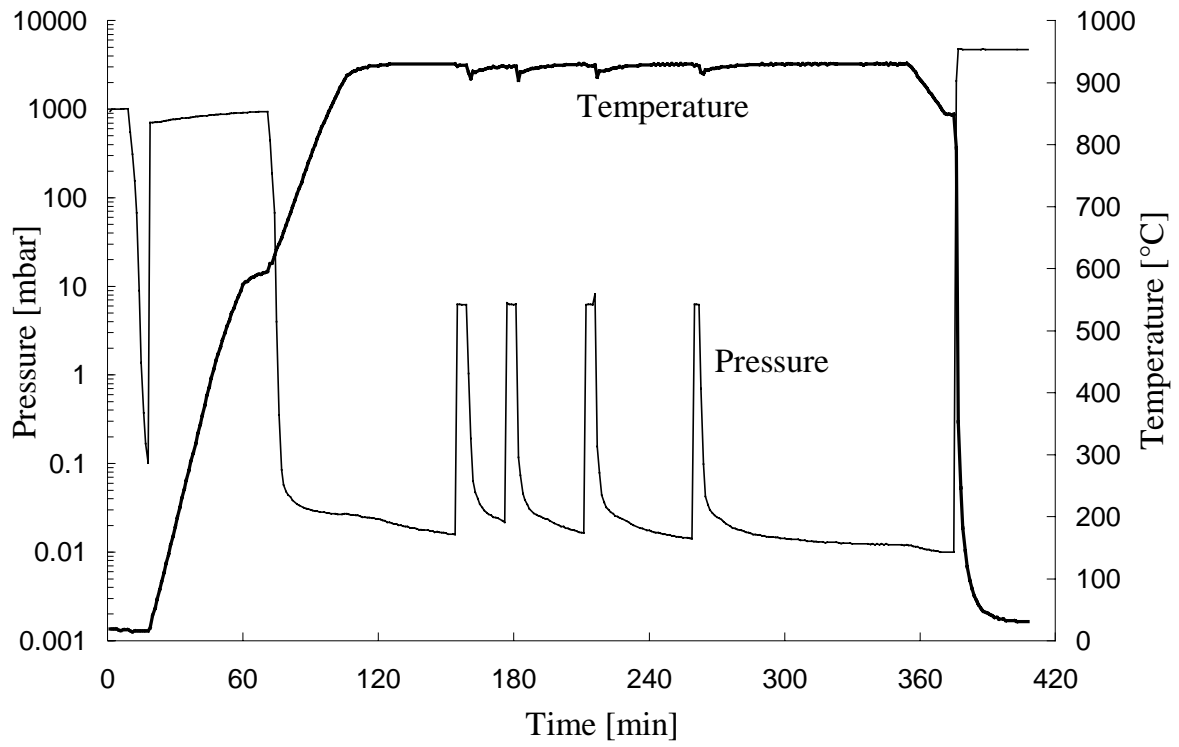


Figure 2: A typical vacuum carburizing cycle with four boost-diffuse steps.

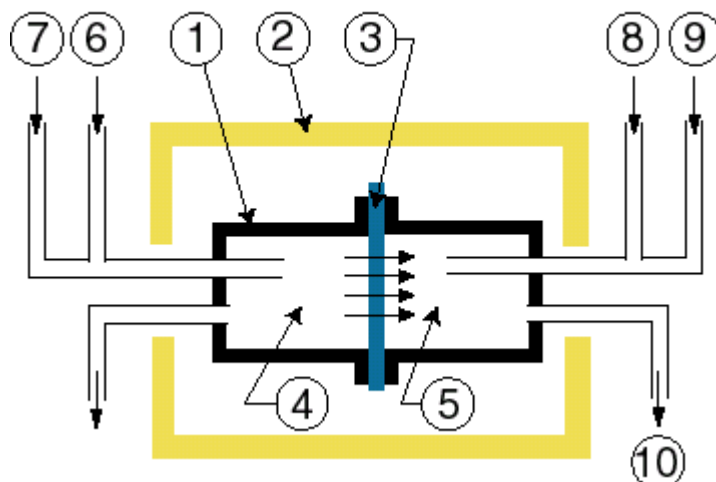


Figure 3: Experimental set-up used to test the concept of the sensor at atmospheric pressure.

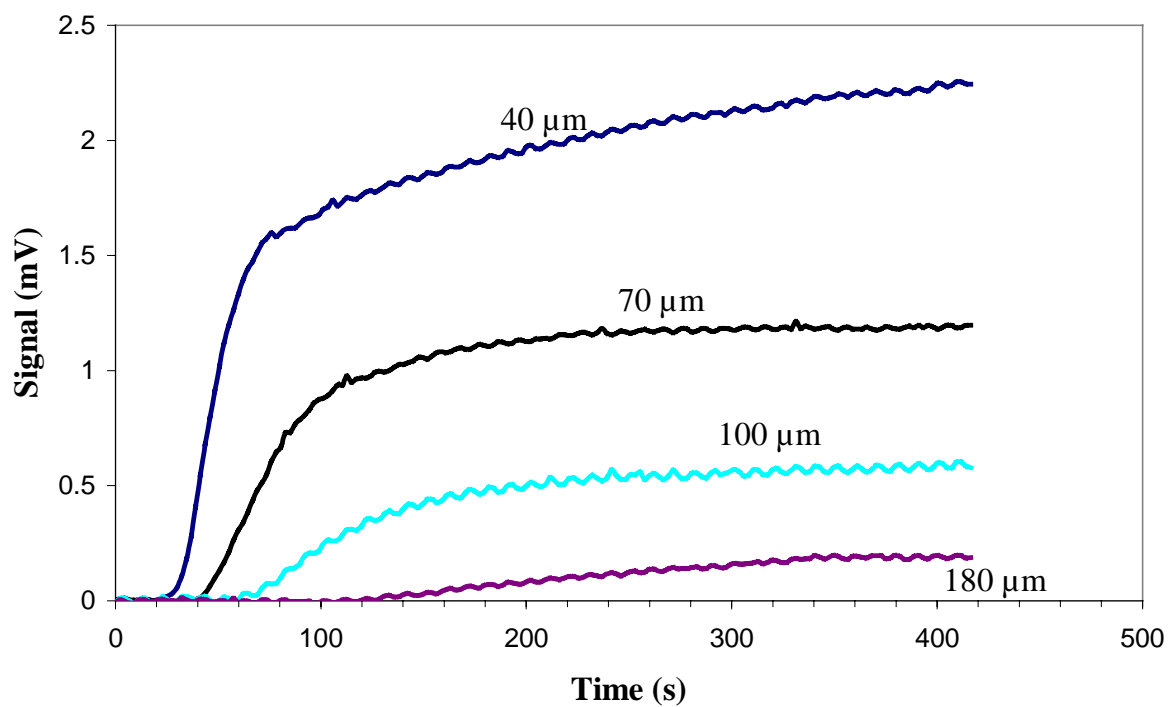


Figure 4: Foil thickness effect on the mass flow rate of carbon and response time.

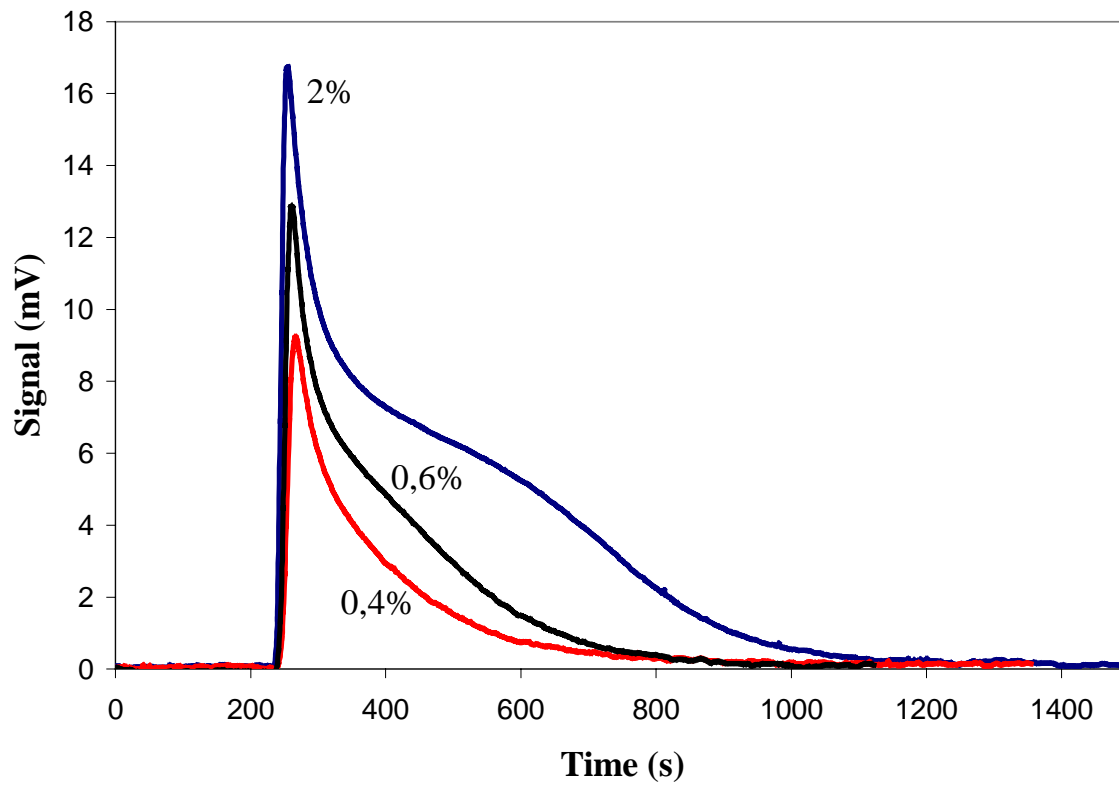


Figure 5: Carburizing gas concentration effect on the mass flow rate of carbon.

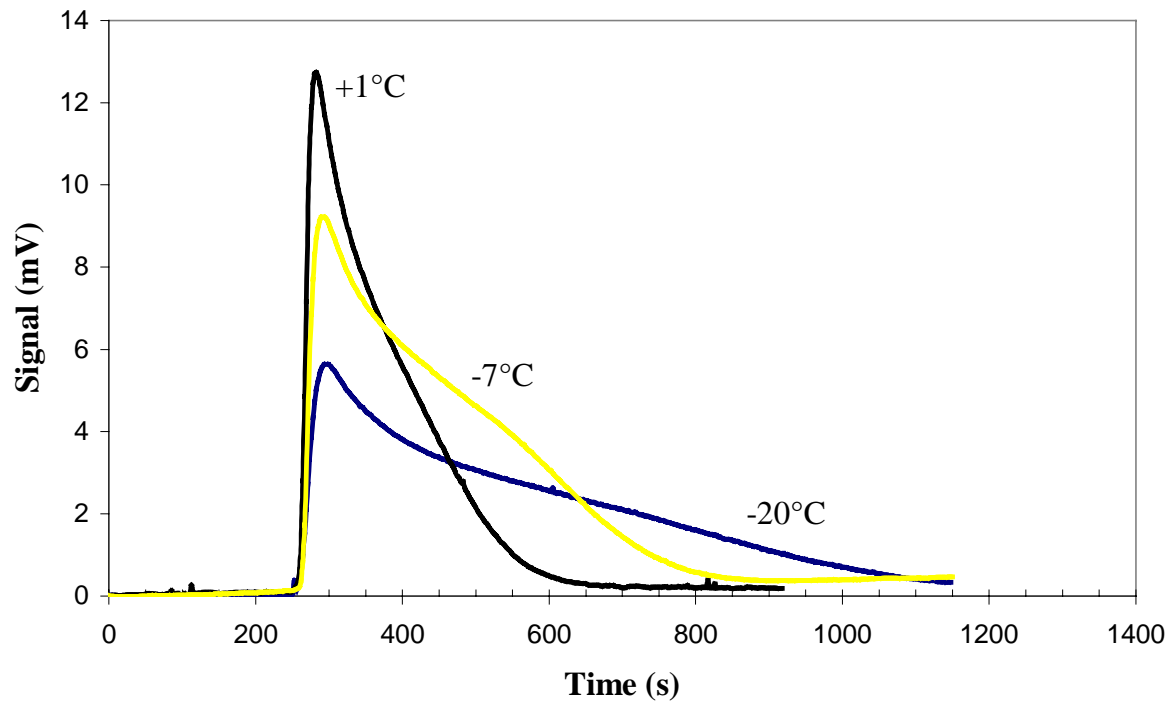


Figure 6: Decarburizing gas composition effect on the mass flow rate of carbon.

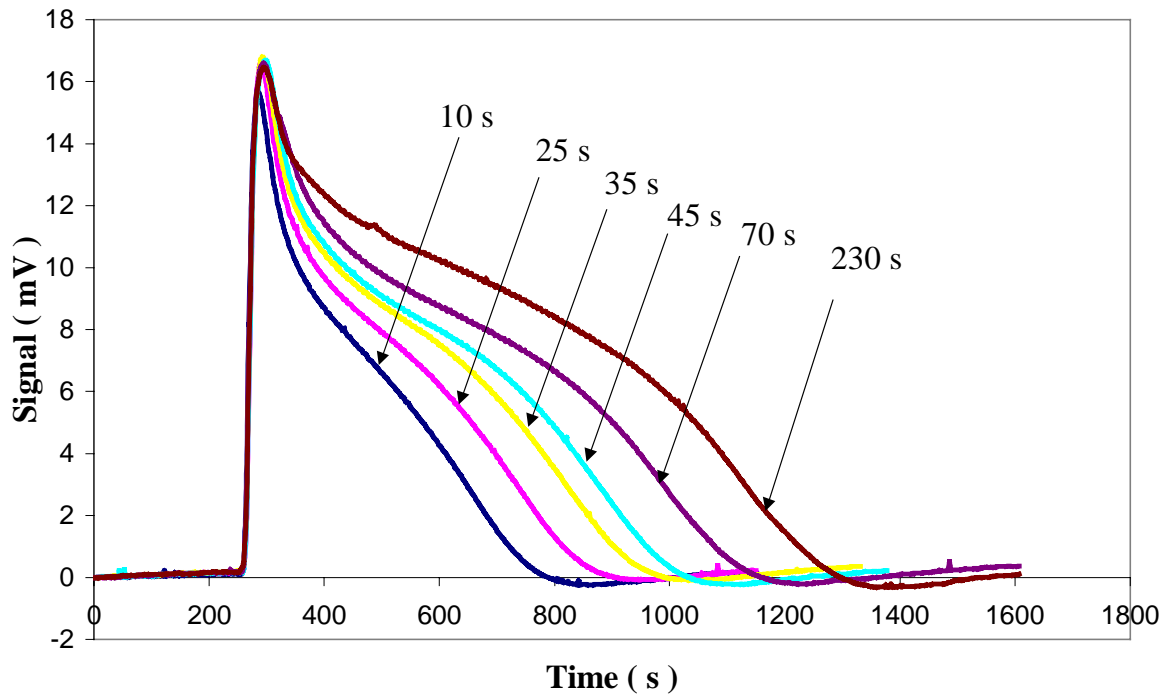


Figure 7: Carburizing period effect on the mass flow rate of carbon.